



**HAL**  
open science

# Transmissibility of nonlinear output frequency response functions with application in detection and location of damage in MDOF structural systems

Z.Q. Lang, G. Park, C.R. Farrar, M.D. Todd, Z. Mao, L. Zhao, K. Worden

► **To cite this version:**

Z.Q. Lang, G. Park, C.R. Farrar, M.D. Todd, Z. Mao, et al.. Transmissibility of nonlinear output frequency response functions with application in detection and location of damage in MDOF structural systems. *International Journal of Non-Linear Mechanics*, 2011, 10.1016/j.ijnonlinmec.2011.03.009 . hal-00753958

**HAL Id: hal-00753958**

**<https://hal.science/hal-00753958>**

Submitted on 20 Nov 2012

**HAL** is a multi-disciplinary open access archive for the deposit and dissemination of scientific research documents, whether they are published or not. The documents may come from teaching and research institutions in France or abroad, or from public or private research centers.

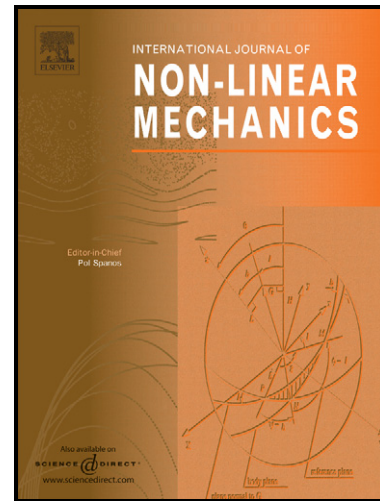
L'archive ouverte pluridisciplinaire **HAL**, est destinée au dépôt et à la diffusion de documents scientifiques de niveau recherche, publiés ou non, émanant des établissements d'enseignement et de recherche français ou étrangers, des laboratoires publics ou privés.

# Author's Accepted Manuscript

Transmissibility of nonlinear output frequency response functions with application in detection and location of damage in MDOF structural systems

Z.Q. Lang, G. Park, C.R. Farrar, M.D. Todd, Z. Mao, L. Zhao, K. Worden

PII: S0020-7462(11)00033-3  
DOI: doi:10.1016/j.ijnonlinmec.2011.03.009  
Reference: NLM1825



[www.elsevier.com/locate/nlm](http://www.elsevier.com/locate/nlm)

To appear in: *International Journal of Non-Linear Mechanics*

Received date: 19 June 2010  
Accepted date: 20 March 2011

Cite this article as: Z.Q. Lang, G. Park, C.R. Farrar, M.D. Todd, Z. Mao, L. Zhao and K. Worden, Transmissibility of nonlinear output frequency response functions with application in detection and location of damage in MDOF structural systems, *International Journal of Non-Linear Mechanics*, doi:[10.1016/j.ijnonlinmec.2011.03.009](https://doi.org/10.1016/j.ijnonlinmec.2011.03.009)

This is a PDF file of an unedited manuscript that has been accepted for publication. As a service to our customers we are providing this early version of the manuscript. The manuscript will undergo copyediting, typesetting, and review of the resulting galley proof before it is published in its final citable form. Please note that during the production process errors may be discovered which could affect the content, and all legal disclaimers that apply to the journal pertain.

# Transmissibility of Nonlinear Output Frequency Response Functions with Application in Detection and Location of Damage in MDOF Structural Systems

Z Q Lang<sup>1</sup>, G Park<sup>2</sup>, C R Farrar<sup>2</sup>, M D Todd<sup>3</sup>, Z Mao<sup>3</sup>, L Zhao<sup>1</sup>, and K Worden<sup>4</sup>

<sup>1</sup>Department of Automatic Control and Systems Engineering, University of Sheffield, Mappin Street, Sheffield, S1 3JD, UK

<sup>2</sup>The Engineering Institute, Los Alamos National Laboratory, MS T-001, Los Alamos, NM 87545 USA

<sup>3</sup>Department of Structural Engineering, University of California San Diego, La Jolla, California 92093-0085, USA

<sup>4</sup>Department of Mechanical Engineering, University of Sheffield, Mappin Street, Sheffield, S1 3JD, UK

## Abstract

Transmissibility is a well-known linear system concept that has been widely applied in the diagnosis of damage in various engineering structural systems. However, in engineering practice, structural systems can behave nonlinearly due to certain kinds of damage such as, e.g., breathing cracks. In the present study, the concept of transmissibility is extended to the nonlinear case by introducing the Transmissibility of Nonlinear Output Frequency Response Functions (NOFRFs). The NOFRFs are a concept recently proposed by the authors for the analysis of nonlinear systems in the frequency domain. A NOFRF transmissibility-based technique is then developed for the detection and location of both linear and nonlinear damage in MDOF structural systems. Numerical simulation results verify the effectiveness of the new technique. Experimental studies on a three-storey building structure demonstrate the potential to apply the developed technique to the detection and location of damage in practical MDOF engineering structures.

Keywords: Transmissibility; Nonlinear MDOF systems; Damage detection and location.

## 1. Introduction

A wealth of methods exists for the detection and location of damage in structural systems. These methods include time and frequency domain techniques, parametric and nonparametric approaches, and empirical and model-based approaches for plates, shells, composites, and other types of structures [1]. The core idea of most of these available techniques is to compare some features evaluated from on-line measured structural responses to the features evaluated from responses measured under the systems' normal working conditions, to assess whether damage has occurred and, if this is the case, where the damage is located.

The frequency-domain transmissibility function is a significant feature that can be applied to detect, locate, and quantify damage in multi-degree of freedom (MDOF) structural systems where structural dynamic sensor arrays can be used to make differential dynamic transmissibility measurements [2]. For MDOF structures, structural damage affects both the system poles and zeros. But, as analysed in [2] and [3], zeros are much more sensitive than poles to localised damage, as zeros depend on the input and output locations whereas poles do not. Transmissibility functions are determined solely by the system zeros, and they are therefore potentially better indicators of localised damage.

The frequency-domain transmissibility function is essentially a linear system concept. It is normally defined as the ratio of the spectra of two different system outputs of interest, and is also equal to the ratio of the system frequency response functions (FRFs) associated with the two outputs. Although, as demonstrated by numerical studies in [2], this transmissibility concept can sometimes be used for the detection and location of damage in nonlinear structural systems, the concept is generally input-dependent for nonlinear systems. Consequently, one is generally not able to use the traditional transmissibility function to distinguish the effect of system input from the effect of the change of system properties due to the occurrence of damage in nonlinear structural systems.

In structural systems, certain types of damage often manifest themselves as the introduction of a nonlinearity into an otherwise linear system [4]. Examples include post-buckled structures (Duffing nonlinearity), rattling joints (impacting system with

discontinuities), or breathing cracks (bilinear stiffness). Therefore effective techniques are needed which can reliably detect and locate both these types of nonlinear damage as well as linear changes due to damage (e.g., a stiffness or mass change, such as with corrosion or loss of an element). Many researchers have addressed different aspects of this important issue using different approaches. These approaches include, for example, mutual information and transfer entropy-based statistical nonlinearity detection methods [4-8], auto-bispectral analysis [9-10], nonlinear system identification techniques [11], and frequency domain ARX model based technique [12]. For MDOF structural systems which include beams, rotor shafts, multi-storey buildings, and bridges, etc. [13,14,15,16,17], damage detection has been studied by Zhu and Wu [18] where the structure with damage is considered to be linear, and the location and magnitude of the damage are estimated using measured changes in the system natural frequencies. Based on a one-dimensional structural model, Sakellariou and Fassois [19] [16] have used a stochastic output-error vibration-based methodology to detect damage in structures where the damaged elements are modeled as components of cubic stiffness. Recently, using the concept of Nonlinear Output Frequency Response Functions (NOFRFs) [20], several methods have been developed which use the response signals to deterministic inputs including sinusoids to detect and locate nonlinear damage in MDOF structural systems [21,22,23,27]. The basic principle and effectiveness of these methods have been verified by theoretical analysis and numerical simulation.

The objective of the present study is to extend the frequency-domain transmissibility-based damage detection and location technique to the nonlinear case to systematically develop a more general transmissibility analysis-based damage detection and location approach for MDOF structural systems. The basis of this study is a new transmissibility concept known as the transmissibility of the NOFRFs.

The NOFRFs are a new concept recently proposed and comprehensively investigated by the authors for the analysis of nonlinear systems in the frequency domain [20]. The concept of the transmissibility of the NOFRFs is defined as the ratio of the maximum order NOFRFs associated with two different output responses of interest in a nonlinear system. For the MDOF structural systems considered in the present study, it is proven that the NOFRF transmissibility is equal to the traditional transmissibility under certain

conditions but is generally different from the traditional transmissibility. However, the NOFRF transmissibility only depends on the system linear characteristics and therefore does not change with the system input. This excellent property of the NOFRF transmissibility is exploited in the present study to develop a new technique that can detect and locate both linear and nonlinear damage in MDOF structural systems. In addition to theoretical derivation and analysis, both numerical simulation studies and experimental tests are conducted in the present study. The results verify the effectiveness of the new technique and demonstrate that the technique has considerable potential to be applied in damage detection and location for real engineering structures.

## 2. Transmissibility of Nonlinear Output Frequency Response Functions

Consider the class of single-input multiple-output (SIMO) nonlinear systems which are stable at zero equilibrium with the outputs represented, in a neighbourhood of the equilibrium, by the Volterra series [25]

$$x_i(t) = \sum_{\bar{n}=1}^N \int_{-\infty}^{\infty} \cdots \int_{-\infty}^{\infty} h_{(i,\bar{n})}(\tau_1, \dots, \tau_{\bar{n}}) \prod_{i=1}^{\bar{n}} u(t - \tau_i) d\tau_i \quad \text{for } i=1, \dots, n \quad (1)$$

In equation (1),  $n$  is the number of the system outputs,  $u(t)$  and  $x_i(t)$  are the input and the  $i^{\text{th}}$  output of the system,  $h_{(i,\bar{n})}(\tau_1, \dots, \tau_{\bar{n}})$  is the  $\bar{n}^{\text{th}}$  order Volterra kernel associated with the  $i^{\text{th}}$  system output, and  $N$  denotes the maximum order of the system nonlinearity.

The output frequency responses of this class of nonlinear systems to a general input can be described as [24]

$$\begin{cases} X_i(j\omega) = \sum_{\bar{n}=1}^N X_{(i,\bar{n})}(j\omega) & \text{for } \forall \omega \\ X_{(i,\bar{n})}(j\omega) = \frac{1/\sqrt{\bar{n}}}{(2\pi)^{\bar{n}-1}} \int_{\omega_1 + \dots + \omega_{\bar{n}} = \omega} H_{(i,\bar{n})}(j\omega_1, \dots, j\omega_{\bar{n}}) \prod_{i=1}^{\bar{n}} U(j\omega_i) d\sigma_{\bar{n}\omega} \end{cases} \quad (2)$$

where  $X_i(j\omega)$  is the spectrum of the  $i^{\text{th}}$  system output,  $X_{(i,\bar{n})}(j\omega)$  represents the  $\bar{n}^{\text{th}}$  order frequency response of the system's  $i^{\text{th}}$  output,  $U(j\omega)$  is the spectrum of the system input, and

$$H_{(i,\bar{n})}(j\omega_1, \dots, j\omega_{\bar{n}}) = \int_{-\infty}^{\infty} \dots \int_{-\infty}^{\infty} h_{(i,\bar{n})}(\tau_1, \dots, \tau_{\bar{n}}) e^{-(\omega_1\tau_1 + \dots + \omega_{\bar{n}}\tau_{\bar{n}})j} d\tau_1 \dots d\tau_{\bar{n}} \quad (3)$$

is known as the  $\bar{n}$ <sup>th</sup> order Generalised Frequency Response Function (GFRF) associated with the  $i$ <sup>th</sup> system output, which is the extension of the frequency response functions of SIMO linear systems to the  $\bar{n}$ <sup>th</sup> order nonlinear case. The term

$$\int_{\omega_1 + \dots + \omega_{\bar{n}} = \omega} H_{(i,\bar{n})}(j\omega_1, \dots, j\omega_{\bar{n}}) \prod_{i=1}^{\bar{n}} U(j\omega_i) d\sigma_{\bar{n}\omega}$$

in equation (2) denotes the integration of  $H_{(i,\bar{n})}(j\omega_1, \dots, j\omega_{\bar{n}}) \prod_{i=1}^{\bar{n}} U(j\omega_i)$  over the  $\bar{n}$ -dimensional hyper-plane  $\omega_1 + \dots + \omega_{\bar{n}} = \omega$ .

The Nonlinear Output Frequency Response Functions (NOFRFs) are a concept recently introduced by the authors [20]. For SIMO nonlinear systems, the NOFRFs are defined as

$$G_{(i,\bar{n})}(j\omega) = \frac{\int_{\omega_1 + \dots + \omega_{\bar{n}} = \omega} H_{(i,\bar{n})}(j\omega_1, \dots, j\omega_{\bar{n}}) \prod_{i=1}^{\bar{n}} U(j\omega_i) d\sigma_{\bar{n}\omega}}{\int_{\omega_1 + \dots + \omega_{\bar{n}} = \omega} \prod_{i=1}^{\bar{n}} U(j\omega_i) d\sigma_{\bar{n}\omega}} \quad \bar{n} = 1, \dots, N \quad (4)$$

under the condition that

$$U_{\bar{n}}(j\omega) = \int_{\omega_1 + \dots + \omega_{\bar{n}} = \omega} \prod_{i=1}^{\bar{n}} U(j\omega_i) d\sigma_{\bar{n}\omega} \neq 0 \quad (5)$$

The NOFRFs defined by equation (4) can be regarded as an alternative extension of the frequency response functions of SIMO linear systems to the  $\bar{n}$ <sup>th</sup> order nonlinear case. The most distinctive characteristic of the NOFRFs is their one dimensional nature, which can significantly facilitate the analysis of nonlinear systems in the frequency domain [28-30].

From equations (2) and (4), it can be shown that the output frequency response of SIMO nonlinear systems can be represented using the NOFRFs as

$$X_i(j\omega) = \sum_{\bar{n}=1}^N X_{(i,\bar{n})}(j\omega) = \sum_{\bar{n}=1}^N G_{(i,\bar{n})}(j\omega) U_{\bar{n}}(j\omega), \quad i=1, \dots, n, \quad (6)$$

For SIMO linear systems,  $N=1$ . So equation (6) reduces to

$$X_i(j\omega) = X_{(i,1)}(j\omega) = G_{(i,1)}(j\omega)U_1(j\omega) = H_{(i,1)}(j\omega)U(j\omega) \quad i=1,\dots,n, \quad (7)$$

where

$$U_1(j\omega) = \int_{\omega_1=\omega} U(j\omega_1) d\sigma_{1\omega} = U(j\omega) \quad (8)$$

$$G_{(i,1)}(j\omega) = \frac{\int_{\omega_1=\omega} H_{(i,1)}(j\omega_1)U(j\omega_1)\sigma_{1\omega}}{\int_{\omega_1=\omega} U(j\omega_1)d\sigma_{1\omega}} = H_{(i,1)}(j\omega) \quad i=1,\dots,n, \quad (9)$$

with  $H_{(i,1)}(j\omega)$ ,  $i=1,\dots,n$ , denoting the frequency response functions (FRFs) of the system. Therefore, equation (6) is an extension of the well-known linear system relationship (7) to the nonlinear case.

Considering that the transmissibility of SIMO linear systems are normally defined as

$$T_{i,k}^L(j\omega) = \frac{H_{(i,1)}(j\omega)}{H_{(k,1)}(j\omega)} = \frac{G_{(i,1)}(j\omega)}{G_{(k,1)}(j\omega)} \quad (10)$$

where  $i,k \in \{1,2,\dots,n\}$  and  $i < k$ , the concept of the transmissibility of the NOFRFs is proposed to extend the linear system transmissibility concept to the nonlinear case as follows.

**Definition:**

*For signal input multi output nonlinear systems, the transmissibility of the NOFRFs between the  $i^{\text{th}}$  and  $k^{\text{th}}$  system outputs is defined as*

$$T_{i,k}^{NL}(j\omega) = \frac{G_{(i,N)}(j\omega)}{G_{(k,N)}(j\omega)} \quad (11)$$

where  $i,k \in \{1,2,\dots,n\}$  and  $i < k$ .

Obviously, when the system is linear, i.e.,  $N=1$ ,

$$T_{i,k}^{NL}(j\omega) = \frac{G_{(i,1)}(j\omega)}{G_{(k,1)}(j\omega)} = T_{i,k}^L(j\omega) \quad (12)$$

that is, the transmissibility of the NOFRFs defined above reduces to the traditional transmissibility of linear systems. In addition, as the NOFRFs are independent of the change of the system input amplitude, the NOFRF transmissibility also does not change with the amplitude. This is the same as the property of the transmissibility of linear systems.

### 3. The NOFRF Transmissibility of MDOF Nonlinear Structural Systems

#### 3.1 MDOF nonlinear structural systems

Consider the multi-degree-of-freedom structural system shown in Fig. 1. For the simplicity of introducing the main ideas, assume that there is only one possible nonlinear component located between the  $(J-1)^{\text{th}}$  and  $J^{\text{th}}$  masses in the system with  $J \in \{2, \dots, n\}$ ; the input force  $u(t)$  is applied at the  $n^{\text{th}}$  mass; and the motion of all the masses is one-dimensional. In addition, it is assumed that the restoring forces of the nonlinear spring and damper, denoted by  $FS(\Delta(t))$  and  $FD(\dot{\Delta}(t))$ , can be any continuous nonlinear functions of the deformation  $\Delta(t) = (x_J(t) - x_{J-1}(t))$  and its derivative  $\dot{\Delta}(t)$ , respectively. Thus by denoting

$$NF(t) = \left( \overbrace{0, \dots, 0}^{J-2}, FS(\Delta(t)) + FD(\dot{\Delta}(t)), -FS(\Delta(t)) - FD(\dot{\Delta}(t)), \overbrace{0, \dots, 0}^{n-J} \right)' \quad (13)$$

and

$$F(t) = \left( \overbrace{0, \dots, 0}^{n-1}, u(t) \right)' \quad (14)$$

the MDOF nonlinear structural system can be described as

$$M\ddot{x}(t) + C\dot{x}(t) + Kx(t) = NF(t) + F(t) \quad (15)$$

where  $x(t) = [x_1(t), \dots, x_n(t)]'$  is the displacement vector, and

$$M = \begin{bmatrix} m_1 & 0 & \cdots & 0 \\ 0 & m_2 & \cdots & 0 \\ \vdots & \vdots & \ddots & \vdots \\ 0 & 0 & \cdots & m_n \end{bmatrix}$$

$$C = \begin{bmatrix} c_1 + c_2 & -c_2 & 0 & \cdots & 0 \\ -c_2 & c_2 + c_3 & -c_3 & \ddots & \vdots \\ 0 & \ddots & \ddots & \ddots & 0 \\ \vdots & \ddots & -c_{n-1} & c_{n-1} + c_n & -c_n \\ 0 & \cdots & 0 & -c_n & c_n \end{bmatrix}$$

$$K = \begin{bmatrix} k_1 + k_2 & -k_2 & 0 & \cdots & 0 \\ -k_2 & k_2 + k_3 & -k_3 & \ddots & \vdots \\ 0 & \ddots & \ddots & \ddots & 0 \\ \vdots & \ddots & -k_{n-1} & k_{n-1} + k_n & -k_n \\ 0 & \cdots & 0 & -k_n & k_n \end{bmatrix}$$

are the system mass, damping, and stiffness matrices, respectively.

### 3.2 The NOFRF transmissibility and properties

The MDOF system described by equation (15) can clearly be regarded as a one-input  $n$ -output system. The system input is the force applied to the  $n^{\text{th}}$  mass  $u(t)$ , and outputs are the displacements of the  $n$  masses. Therefore, denote the output spectra of the  $i^{\text{th}}$  and  $k^{\text{th}}$  masses in the system as  $X_i(j\omega)$  and  $X_k(j\omega)$ , then  $X_i(j\omega)$  and  $X_k(j\omega)$  can be described using the NOFRF concepts as

$$X_i(j\omega) = \sum_{\bar{n}=1}^N G_{(i,\bar{n})}(j\omega) U_{\bar{n}}(j\omega) \quad (16)$$

and

$$X_k(j\omega) = \sum_{\bar{n}=1}^N G_{(k,\bar{n})}(j\omega) U_{\bar{n}}(j\omega) \quad (17)$$

respectively where  $G_{(i,\bar{n})}(j\omega)$  and  $G_{(k,\bar{n})}(j\omega)$  are the  $\bar{n}$ th order NOFRFs associated with the displacements of the  $i^{\text{th}}$  and  $k^{\text{th}}$  masses of the system, and  $U_{\bar{n}}(j\omega)$  is defined in equation (5) with  $U(j\omega)$  representing the spectrum of the input force  $u(t)$ .

In this case, the NOFRF transmissibility  $T_{i,k}^{NL}(j\omega)$  defined in equation (11) refers to the transmissibility between the displacements of masses  $i$  and  $k$  in the MDOF structural

system; and  $T_{i,k}^L(j\omega)$  defined in equation (10) represents the ratio between the 1<sup>st</sup> order NOFRFs associated with the displacements of the  $i^{\text{th}}$  and  $k^{\text{th}}$  masses. Based on these definitions, a series of properties regarding the NOFRF transmissibility of the MDOF structural system (15) can be obtained. These are summarized in the following two propositions.

#### Proposition 1

For system (15),  $T_{i,k}^{NL}(j\omega)$  and  $T_{i,k}^L(j\omega)$  are completely determined by the system linear characteristic parameters M, C, and K as follows

$$T_{i,k}^{NL}(j\omega) = \prod_{z=i}^{k-1} \frac{Q_{z,J-1}(j\omega) - Q_{z,J}(j\omega)}{Q_{z+1,J-1}(j\omega) - Q_{z+1,J}(j\omega)} \quad (18)$$

$$T_{i,k}^L(j\omega) = \prod_{z=i}^{k-1} \frac{Q_{(z,n)}(j\omega)}{Q_{(z+1,n)}(j\omega)} \quad (19)$$

where

$$\begin{bmatrix} Q_{(1,1)}(j\omega) & \cdots & Q_{(1,n)}(j\omega) \\ \vdots & \ddots & \vdots \\ Q_{(n,1)}(j\omega) & \cdots & Q_{(n,n)}(j\omega) \end{bmatrix} = (-M\omega^2 + jC\omega + K)^{-1}$$

In addition

$$T_{i,k}^{NL}(j\omega) = \frac{G_{(i,\bar{n})}(j\omega)}{G_{(k,\bar{n})}(j\omega)} \quad \text{where } 2 \leq \bar{n} \leq N \quad (20)$$

and there exist the following relationships between  $T_{i,k}^{NL}(j\omega)$  and  $T_{i,k}^L(j\omega)$

$$\begin{cases} T_{i,k}^{NL}(j\omega) = T_{i,k}^L(j\omega) & \text{if } 1 \leq i < k \leq J-1 \\ T_{i,k}^{NL}(j\omega) \neq T_{i,k}^L(j\omega) & \text{otherwise} \end{cases} \quad (21)$$

Proof: The conclusions (18)-(21) can be reached by following the derivation for the NOFRF properties of MDOF systems in [26], and taking into account the definitions of  $T_{i,k}^{NL}(j\omega)$  and  $T_{i,k}^L(j\omega)$  introduced above.  $\square$

#### Proposition 2

For system (15), the NOFRF transmissibility  $T_{i,k}^{NL}(j\omega)$  and a function of frequency  $E_{ik}(j\omega)$  defined by

$$E_{i,k}(j\omega) = [G_{(i,1)}(j\omega) - T_{i,k}^{NL}(j\omega)G_{(k,1)}(j\omega)] \quad (22)$$

can be determined from the system input and output spectra as follows;

$$\begin{bmatrix} E_{i,k}(j\omega) \\ T_{i,k}^{NL}(j\omega) \end{bmatrix} = \begin{bmatrix} U^{(1)}(j\omega), & X_k^{(1)}(j\omega) \\ U^{(2)}(j\omega), & X_k^{(2)}(j\omega) \end{bmatrix}^{-1} \begin{bmatrix} X_i^{(1)}(j\omega) \\ X_i^{(2)}(j\omega) \end{bmatrix} \quad (23)$$

if the inverse of matrix

$$\begin{bmatrix} U^{(1)}(j\omega), & X_k^{(1)}(j\omega) \\ U^{(2)}(j\omega), & X_k^{(2)}(j\omega) \end{bmatrix} \quad (24)$$

exists. In (23),  $U^{(1)}(j\omega)$  and  $U^{(2)}(j\omega)$  are the spectra of two different input forces separately applied to the system,  $X_i^{(1)}(j\omega)$  and  $X_k^{(1)}(j\omega)$  are the spectra of the displacement responses of masses  $i$  and  $k$  in the system to the input force with spectrum  $U^{(1)}(j\omega)$ , and  $X_i^{(2)}(j\omega)$  and  $X_k^{(2)}(j\omega)$  are the spectra of the displacement responses of masses  $i$  and  $k$  in the system to the input force with spectrum  $U^{(2)}(j\omega)$ .

Proof: See the Appendix. □

Proposition 1 shows that for system (15), the NOFRF transmissibility  $T_{i,k}^{NL}(j\omega)$  and the ratio of the 1<sup>st</sup> order NOFRFs  $T_{i,k}^L(j\omega)$  are all independent of the system input and completely determined by the system linear characteristic parameters. This property implies that just like the traditional transmissibility concept for linear SIMO systems, the NOFRF transmissibility  $T_{i,k}^{NL}(j\omega)$  can be used to evaluate changes in the linear characteristic parameters of the nonlinear MDOF system (15). In addition, Proposition 1 shows that  $T_{i,k}^{NL}(j\omega)$  equals to the ratio of the higher-than-one order NOFRFs associated with mass 1 and  $k$  (equation (20)), and reveals an important relationship between  $T_{i,k}^{NL}(j\omega)$  and  $T_{i,k}^L(j\omega)$  (equation (21)).

Proposition 2 indicates that under the invertibility condition of matrix (24), the NOFRF transmissibility  $T_{i,k}^{NL}(j\omega)$  of system (15) can be determined using the system input and output spectra obtained from two separate tests. Proposition 2 also shows that  $E_{ik}(j\omega)$  defined in (22) can be obtained using the same system input and output spectra. The significance of  $E_{ik}(j\omega)$  is that it can be used to evaluate the difference between  $T_{i,k}^{NL}(j\omega)$  and  $T_{i,k}^L(j\omega)$ . This is because if  $T_{i,k}^{NL}(j\omega) = T_{i,k}^L(j\omega)$

$$\begin{aligned} E_{i,k}(j\omega) &= [G_{(i,1)}(j\omega) - T_{i,k}^{NL}(j\omega)G_{(k,1)}(j\omega)] \\ &= G_{(k,1)}(j\omega)[T_{i,k}^L(j\omega) - T_{i,k}^{NL}(j\omega)] = 0 \end{aligned} \quad (25)$$

otherwise

$$E_{i,k}(j\omega) \neq 0 \quad (26)$$

in general. This, together with the relationship between  $T_{i,k}^{NL}(j\omega)$  and  $T_{i,k}^L(j\omega)$  revealed in Proposition 1, can be exploited to determine the location of the nonlinear component in the system.

#### 4. A NOFRF Transmissibility-based Technique for the Detection and Location of Damage in MDOF Structural Systems

The introduction of the concept of the NOFRF transmissibility in Section 2 is to address the damage detection and location issue for the MDOF structural system (15). Equation (15) describes a class of MDOF nonlinear structural systems where the nonlinear component can represent damage in the system such as, for example, a crack in a beam. The M, C, and K matrices represent the linear characteristics of the system, and damage in the system can also change the values of these matrices. Therefore, the objectives are to detect the existence of the nonlinear component and locate its position, and to identify any changes in the M, C, and K matrices. These objectives are to be achieved based on the input force and corresponding responses of all the masses in the system which can, for example, be the outputs of an array of sensors fitted to the structure for health monitoring purposes.

The traditional transmissibility concept has already been used in [2] as a differential indicator to detect and locate structural damage. Although some nonlinear damage was also considered in this previous study, the conclusions reached are based on a specific case study and can not be extended to general nonlinear MDOF structural systems. This is simply because the traditional transmissibility is a linear system concept; and the result is input-dependent in the nonlinear case.

In order to resolve the problem with traditional transmissibility concept-based approaches, a NOFRF transmissibility based technique for the detection and location of damage in the MDOF structural system (15) is proposed in this section based on the system NOFRF transmissibility and properties that have been derived in Section 3.2.

The basic ideas of the damage detection and location technique are to apply two different forces to excite the system to get two sets of corresponding system responses. Then, evaluate the spectra of the force excitations and corresponding responses and detect the existence of nonlinear component/damage in the system by checking the invertibility of matrix (24).

This system nonlinearity detection method is based on the fact that if there is no nonlinear component/damage in system (15), the system is linear so that

$$\frac{X_k^{(1)}(j\omega)}{U^{(1)}(j\omega)} = \frac{X_k^{(2)}(j\omega)}{U^{(2)}(j\omega)} \quad (27)$$

and the inverse of matrix (24) does not exist. Consequently, an invertible condition of matrix (24) such as, e.g., whether the determinant of matrix (24) is zero can be used to detect whether there exists a nonlinear component/damage in the system.

After that, if the matrix-invertibility-check indicates that there is no nonlinear component in the system, then the system is linear, and the traditional transmissibility based technique will be applied for the detection and location of possible linear damage in the system. Otherwise, there is a nonlinear damage/component in the system. Equation (23) will be applied to evaluate  $T_{i,i+1}^{NL}(j\omega)$  and  $E_{i,i+1}(j\omega)$  for each pair of consecutive masses in the system, that is, for  $i=1, \dots, n-1$ . Then the NOFRF

transmissibility results  $T_{i,i+1}^{NL}(j\omega)$   $i=1, \dots, n-1$  will be used to evaluate the changes in the system linear characteristic parameters to detect and locate possible linear damage in the system, and  $E_{i,i+1}(j\omega)$ ,  $i=1, \dots, n-1$ , will be used to determine the location of the system nonlinear damage/component.

The theoretical basis of determining the location of the nonlinear component is equations (21) and (22), which imply that

$$\begin{cases} T_{i,i+1}^{NL}(j\omega) = T_{i,i+1}^L(j\omega) \Rightarrow E_{i,i+1}(j\omega) = G_{(i+1,1)}(j\omega)[T_{i,i+1}^L(j\omega) - T_{i,i+1}^{NL}(j\omega)] = 0 \\ \hspace{15em} \text{if } 1 \leq i \leq J-2 \\ T_{i,i+1}^{NL}(j\omega) \neq T_{i,i+1}^L(j\omega) \Rightarrow E_{i,i+1}(j\omega) = G_{(i+1,1)}(j\omega)[T_{i,i+1}^L(j\omega) - T_{i,i+1}^{NL}(j\omega)] \neq 0 \\ \hspace{15em} \text{Otherwise} \end{cases} \quad (28)$$

Therefore, theoretically, the system nonlinear component is located between masses  $i^*$  and  $i^* + 1$  where  $i^*$  is determined by the values of  $|E_{i,i+1}(j\omega)|$ ,  $i=1, \dots, n-1$ , such that

$$\begin{cases} |E_{i,i+1}(j\omega)| > 0 & \text{when } i^* \leq i < n \\ |E_{i,i+1}(j\omega)| = 0 & \text{Otherwise} \end{cases} \quad (29)$$

Based on these ideas and considering various issues associated with real data analysis observed in comprehensive experimental studies that have been conducted by the authors on MDOF test rigs [34], the damage detection and location technique for MDOF structural system (15) is proposed as follows.

- i) Excite the system twice using two different inputs with spectra  $U^{(1)}(j\omega)$  and  $U^{(2)}(j\omega)$ , respectively; Measure the responses of all the masses in the system to each input excitation, and calculate the spectra of the measured responses to obtain  $X_k^{(1)}(j\omega)$ ,  $k=1, \dots, n$ , and  $X_k^{(2)}(j\omega)$ ,  $k=1, \dots, n$ .
- ii) Evaluate index IND1 as defined by

$$\text{IND1} = \frac{1}{(n-1)} \sum_{k=2}^n \text{Median}\{D_k(q\Delta\omega); q = 0, \dots, Q\} \quad (30)$$

where

$$D_k(q\Delta\omega) = \left| \det \begin{bmatrix} U^{(1)}(jq\Delta\omega) & X_k^{(1)}(jq\Delta\omega) \\ U^{(2)}(jq\Delta\omega) & X_k^{(2)}(jq\Delta\omega) \end{bmatrix} \right|$$

$$\Delta\omega = \frac{\omega_2 - \omega_1}{Q}$$

Q is an integer, and  $[\omega_1, \omega_2]$  is an interval within the frequency range of the system input. The result is used to determine whether or not there is a nonlinear component in the system as follows:

*If  $\text{IND}1 \leq \varepsilon_1$ , then the system nonlinearity is negligible;  
otherwise there is a nonlinear component in the system.*

Here  $\varepsilon_1$  is zero in theory (a noise-free environment) but in practice, it should be a small number associated with a noise threshold in a case where the system basically behaves linearly.

- iii) If the result in Step ii) indicates that there is negligible nonlinearity, then evaluate the traditional linear transmissibility between the responses of all consecutive masses to yield

$$T_{i,i+1}^L(j\omega) = \left\{ \frac{X_i^{(1)}(j\omega)}{X_{i+1}^{(1)}(j\omega)} + \frac{X_i^{(2)}(j\omega)}{X_{i+1}^{(2)}(j\omega)} \right\} / 2 \quad i=1, \dots, n-1 \quad (31)$$

over the frequency range  $[\omega_1, \omega_2]$ , and assess the changes in the system linear characteristics by comparing the evaluated  $T_{i,i+1}^L(j\omega)$ ,  $i=1, \dots, n-1$  with the results evaluated in the system normal operating conditions to detect and locate damage that can be deduced from changes in the system linear characteristic parameters

- iv) If the result in Step (ii) indicates that the system is behaving nonlinearly, determine the NOFRF transmissibility  $T_{i,i+1}^{NL}(j\omega)$  and  $E_{i,i+1}(j\omega)$  from equation (23) with  $k=i+1$  over the frequency range  $[\omega_1, \omega_2]$  for  $i=1, \dots, n-1$ . Then, locate the damage that makes the system behave nonlinearly, and assess the state condition of the system linear components using the evaluated NOFRF transmissibility results  $T_{i,i+1}^{NL}(j\omega)$ ,  $i=1, \dots, n-1$  to detect and locate possible damage that induces changes in the system linear components. Locating nonlinear damage can be achieved as follows.

(a) Evaluate

$$E_{i,i+1} = \int_{\omega_1}^{\omega_2} |E_{i,i+1}(j\omega)| d\omega \quad i=1, \dots, n-1$$

(b) Find a normalized result for  $E_{i,i+1}$  as

$$\bar{E}_{i,i+1} = \frac{E_{i,i+1}}{\max_{i \in \{1, \dots, n-1\}} E_{i,i+1}} \quad i=1, \dots, n-1 \quad (32)$$

(c) Examine  $\bar{E}_{i,i+1}$ ,  $i=1, \dots, n-1$  to find an  $\hat{i}$  such that

$$\begin{cases} \bar{E}_{i,i+1} \leq \varepsilon_2 & i < \hat{i} \\ \bar{E}_{i,i+1} > \varepsilon_2 & i = \hat{i} \end{cases} \quad (33)$$

Then, it can be concluded that the nonlinear damage is located between mass  $\hat{i}$  and mass  $\hat{i} + 1$ . In practical applications,  $\varepsilon_2$  in (33) is a specific case-dependent threshold, which can be determined from experimental data using statistic analyses.

Fig 2 shows a flow chart that illustrates how to follow the four-step procedure to implement this NOFRF transmissibility-based MDOF system damage detection and location technique.

Step i) of this technique indicates that two tests are needed for the system inspection, and the force excitations used in the two tests should be different. However, it is worth pointing out that this does not mean the technique needs the data from two specially designed inspecting tests. In fact, the data collected from two inspecting conditions where the input forces from ambient environment are different should also be sufficient for the implementation of the technique. Step ii) is a practical implementation of the idea of detecting the existence of nonlinearity in the system based on the invertible condition of matrix (24). It is worth noting that the median function is used in this implementation to avoid outlying values of the determinant at some frequencies caused by noise or other disturbances affecting the analysis results in practice. Step (iii) is a traditional transmissibility analysis based procedure, which detects and locates the system damage by evaluating the changes in the system linear characteristic parameters. In Step (iv),  $\bar{E}_{i,i+1}$ ,  $i=1, \dots, n-1$ , which are the normalized results of  $E_{i,i+1}$ ,

$i=1, \dots, n-1$ , are used to implement the equation (29) based idea of determining the location of nonlinear damage. A threshold of  $\varepsilon_2 > 0$  is introduced in this step to change the purely theoretical condition of  $\bar{E}_{i,i+1} = 0$  to the more practical condition of  $\bar{E}_{i,i+1} \leq \varepsilon_2$ . This allows the effects of noise, un-modeled dynamics, and inherent but less significant system nonlinearities to be omitted in the detection of the relatively considerable system nonlinearity so that the proposed method can be applied in engineering practice. In addition, by exploiting the fact that NOFRF transmissibility  $T_{i,i+1}^{NL}(j\omega)$ ,  $i=1, \dots, n-1$  are completely determined by the characteristics of the system linear components, Step (iv) also assesses the state condition of the system linear components using the evaluated NOFRF transmissibility to detect and locate possible linear damage.

In the authors' previous studies, a series of techniques [21,22,23,27] have been proposed for the location of nonlinear damage in MDOF structural systems. Most of these previous techniques [22, 23, 27] require to test an inspected structure using specific inputs. These can be achieved in well controlled test conditions but are difficult for many practical situations. We realized the problems when processing experimental data using these techniques and this motivated us to develop the new technique introduced above. The new technique only needs the system excitation and response data collected under two different loading conditions, and this requirement can be satisfied even for the cases where only ambient excitations to the system are available. In addition, via the introduction of the NOFRF transmissibility concept, the new technique significantly extends the nonlinearity location method for MDOF systems in [21]. This is because the new technique provides a comprehensive procedure, which can not only be used to detect the existence of nonlinear damage and find its location, but is also able to detect and locate damage that can induce changes in the system linear characteristic parameters.

## 5. Simulation Studies on a 3DOF Structural System

In this section, numerical simulation studies on a 3DOF system (i.e.  $n=3$  in Fig 1), where the characteristic of the third spring can be nonlinear (i.e.,  $J=3$ ), are conducted to demonstrate the effectiveness of the technique proposed in the last Section.

Consider the 3DOF system in four different specific cases as follows:

Case I:

$$m_1 = m_2 = m_3 = 1\text{kg}; \quad k_1 = k_2 = k_3 = 3.6 \times 10^4 \text{ (N/m)};$$

$$c_1 = c_2 = c_3 = 0.01 \times 3.6 \times 10^4 \text{ (Ns/m)};$$

There is no nonlinear component in the system.

Case II:

$$m_1 = m_2 = m_3 = 1\text{kg}; \quad k_1 = k_2 = k_3 = 3.6 \times 10^4 \text{ (N/m)};$$

$$c_1 = c_2 = c_3 = 0.01 \times 3.6 \times 10^4 \text{ (Ns/m)};$$

The third spring is nonlinear, i.e.,  $J=3$ , with its restoring force given by

$$FS(x_3 - x_2) = \sum_{l=1}^2 r_l (x_3 - x_2)^l = k_3 (x_3 - x_2) + 0.01 \times k_3^2 (x_3 - x_2)^2.$$

Case III:

$$m_1 = m_2 = m_3 = 1\text{kg}; \quad k_1 = 2 \times 10^4 \text{ (N/m)}; \quad k_2 = k_3 = 3.6 \times 10^4 \text{ (N/m)}$$

$$c_1 = c_2 = c_3 = 0.01 \times 3.6 \times 10^4 \text{ (Ns/m)};$$

The third spring is nonlinear, i.e.,  $J=3$ , with its restoring force given by

$$FS(x_3 - x_2) = \sum_{l=1}^2 r_l (x_3 - x_2)^l = k_3 (x_3 - x_2) + 0.01 \times k_3^2 (x_3 - x_2)^2.$$

Case IV

$$m_1 = m_2 = m_3 = 1\text{kg}; \quad k_3 = 0.5 \times 3.6 \times 10^4 \text{ (N/m)}; \quad k_1 = k_2 = 3.6 \times 10^4 \text{ (N/m)}$$

$$c_1 = c_2 = c_3 = 0.01 \times 3.6 \times 10^4 \text{ (Ns/m)};$$

The third spring is nonlinear, i.e.,  $J=3$ , with its restoring force given by

$$FS(x_3 - x_2) = \sum_{l=1}^2 r_l (x_3 - x_2)^l = k_3 (x_3 - x_2) + 0.01 \times k_2^2 (x_3 - x_2)^2.$$

The technique proposed in Section 4 was applied to the 3DOF system in the four cases, respectively. In all these cases, the applied force excitations were the same, which are

$$u_1(t) = \sin(2\pi \times 20 \times t + \pi/6) + 20 \times \sin(2\pi \times 20 \times t) \quad \text{and} \quad u_2(t) = 2u_1(t)$$

For each case, the displacements of the three masses in the system,  $x_i(t), i = 1, 2, 3$ , were obtained by numerical simulation, and the applied inputs and numerically simulated system displacement responses were used to determine

$$\text{IND1} = \frac{1}{2} \sum_{k=2}^3 D_k (2 \times \pi \times 20)$$

where  $D_k (2 \times \pi \times 20) = \left| \det \begin{bmatrix} U^{(1)}(j2 \times \pi \times 20) & X_k^{(1)}(j2 \times \pi \times 20) \\ U^{(2)}(j2 \times \pi \times 20) & X_k^{(2)}(j \times \pi \times 20) \end{bmatrix} \right|$ ,  $k=2, 3$ , and

$$E_{1,2} = |E_{1,2}(j2 \times \pi \times 20)|$$

$$E_{2,3} = |E_{2,3}(j2 \times \pi \times 20)|$$

$$\bar{E}_{1,2} = \frac{E_{1,2}}{\max_{i \in \{1,2\}} E_{i,i+1}},$$

$$\bar{E}_{2,3} = \frac{E_{2,3}}{\max_{i \in \{1,2\}} E_{i,i+1}},$$

$$|T_{1,2}^{NL}(j\omega)| = |T_{1,2}^{NL}(j2 \times \pi \times 20)|,$$

$$|T_{2,3}^{NL}(j\omega)| = |T_{2,3}^{NL}(j2 \times \pi \times 20)|.$$

in order to detect the existence and find the location of the nonlinear component in the system (from  $\text{IND1}$ ,  $\bar{E}_{1,2}$ , and  $\bar{E}_{2,3}$ ) and evaluate the characteristics of the system linear components (from  $E_{1,2}$ ,  $E_{2,3}$ ,  $|T_{1,2}^{NL}(j\omega)|$ , and  $|T_{2,3}^{NL}(j\omega)|$ ).

Tables 1-4 show the numerical analysis results obtained together with the theoretical values of these results.

From Table 1, it is known that the value of IND1 is a very small number indicating that the system in Case I was behaving linearly, which is obviously correct. Because of the very small determinant value, the NOFRF transmissibility results were determined using equation (31) in Step iii) of the technique, and no results for  $E_{i,i+1}(j\omega)$   $i=1,\dots,n-1$  were evaluated for this case.

A comparison of the IND1 value in Table 1 with that in Table 2 indicates that the system in Case II was behaving considerably more nonlinearly. The conclusion that there exists a nonlinear component in the system can readily be reached for this case if choosing  $\varepsilon_1 = 10^{-9}$  and comparing IND1 with this threshold.

Moreover, it is known from the results in Table 2 that if choosing  $\varepsilon_2 = 10^{-4}$ , then  $\bar{E}_{23} = 1 > \varepsilon_2$ ,  $\bar{E}_{12} = 0.0000445 < \varepsilon_2$ . This, as described in the proposed technique, indicates that  $\hat{i} = 2$ , that is, the nonlinear component is located between mass  $\hat{i} = 2$  and mass  $\hat{i} + 1 = 3$ , which is obviously correct for Case II. In addition, comparing the results of  $E_{1,2}, E_{2,3}, |T_{12}^{NL}(j\omega)|, |T_{23}^{NL}(j\omega)|$  evaluated using the technique and their theoretical values shows an excellent agreement, which verifies the effectiveness of the system input/output data-based analysis.

A comparison of the results of the NOFRF transmissibility in Tables 1 and 2 shows that the  $|T_{12}^{NL}(j\omega)|$  results are the same but the  $|T_{23}^{NL}(j\omega)|$  results are different in the two tables. This is because there is a nonlinear component located between mass 2 and mass 3 in Case II, the system is completely linear in Case I, and, apart from this difference, the systems in the two cases are the same. Therefore, if the system is normal in Case I, but in addition to nonlinear damage there also exist linear damage in Case II which induces changes in the system parameters that affect  $|T_{12}^{NL}(j\omega)|$ , then the damage can be effectively detected by comparing the  $|T_{12}^{NL}(j\omega)|$  results in the two cases.

The analysis results for Cases III and IV in Tables 3 and 4 further confirm the effectiveness of the proposed technique. In addition, a comparison of the results of  $E_{23}, |T_{12}^{NL}(j\omega)|, |T_{23}^{NL}(j\omega)|$  in Tables 2 and 3 shows that the change of the system parameter  $k_1$  from  $k_1 = 3.6 \times 10^4$  (N/m) in Case II to  $k_1 = 2 \times 10^4$  (N/m) in Case III causes the changes in the evaluated values for  $E_{23}, |T_{12}^{NL}(j\omega)|, |T_{23}^{NL}(j\omega)|$ . This demonstrates the dependence of these results evaluated by the proposed technique on the system characteristic parameter  $k_1$ , and indicates that the proposed technique can be used to detect and evaluate the change in the system parameter  $k_1$ . However, a comparison of the results of  $E_{23}, |T_{12}^{NL}(j\omega)|, |T_{23}^{NL}(j\omega)|$  in Tables 2 and 4 show that the change of the system parameter  $k_3$  from  $k_3 = 3.6 \times 10^4$  (N/m) in Case II to  $k_3 = 0.5 \times 3.6 \times 10^4$  (N/m) in Case IV induces no change in the evaluated values for  $E_{23}, |T_{12}^{NL}(j\omega)|, |T_{23}^{NL}(j\omega)|$ . Because  $k_3$  is a characteristic parameter of the system nonlinear component, this result implies that the NOFRF transmissibility results are completely determined by the characteristics of the system's linear components. Therefore, the NOFRF transmissibility should only be used to evaluate the changes in the system linear components.

## 6. Experimental studies

### 6.1 Experimental setup

The three-storey building structure [31] shown in Fig 3 was used in the study to demonstrate the potential of the proposed NOFRF transmissibility-based technique for the detection and location of damage in practical MDOF structural systems. The structure consists of aluminum columns and plates, assembled using bolted joints with a rigid base. The structure slides on rails that allow movement in only one direction. At each floor, four columns (17.7x2.5x0.6cm) are connected to the top and bottom aluminum plates (30.5x30.5x2.5 cm), which form a four degree-of-freedom system. Additionally, a center column (15.0x2.5x2.5 cm) can be suspended from the top of each floor (Figs 3 and 4 show the case where the column is suspended from the top of the second floor), which is used to induce nonlinear behaviours when the column contacts a

bumper mounted on the next floor. The position of the bumper can be adjusted to vary the extent of the nonlinearity. This source of nonlinearity can, for example, simulate the fatigue cracks that subsequently open and close under operational and environmental conditions. An electromagnetic shaker provides the excitation to the ground floor of the structure. A force transducer was attached at the end of a stinger to measure the input force from the shaker. Four accelerometers are attached to each floor at the opposite side from the excitation source to measure the response from each floor. Fig. 4 shows the spring-damper model of the three-storey building structure which is clearly a specific case of the nDOF model in Fig.1.

## 6.2 Experiments and objectives of experimental data analysis

The data collected from twelve experiments conducted on the structure were analyzed for the present study to evaluate the performance of the proposed damage detection and location technique in different practical situations. The details of the experiments are summarized in Table 5. Six different state conditions of the structure were investigated. These are the structural state conditions under Experiments #1 and #2, Experiments #3 and #4, Experiments #5 and #6, Experiments #7 and #8, Experiments #9 and #10, and Experiments #11 and #12, respectively.

The objectives of the experimental data analysis are to apply the proposed technique to two sets of signals measured by the force transducer and four accelerometers from Experiment  $\#(2i - 1)$  and Experiment  $\#2i$ , respectively, to evaluate state condition  $i$  of the structural system for  $i = 1, 2, 3, 4, 5, 6$ . It is worth pointing out that in the description for the proposed technique in Section 4, the displacement of each degree of freedom in system (15) is considered to be the system output response, it can be shown that the technique will be the same if, instead of displacement, the acceleration is regarded as the system output. Therefore, the proposed technique can directly be applied to process the experimental data from the three-storey building structure for the purposes of damage detection and location.

The analysis results for structural state condition 1 will be compared with the analysis results for structural state condition 2 to examine the difference between the results to see how the introduction of nonlinearity into the system changes the outcome of

analysis. This is to simulate the situation of detecting the existence of nonlinear damage and determining its location. Then, the analysis results for structural state condition 3 will be compared with the analysis results for structural state condition 4 to demonstrate how the changes in the characteristic parameters of linear components in a nonlinear structure can be identified by the analysis. This is to simulate the situation where the proposed technique is applied to a nonlinear structural system and the changes in structural linear components are to be detected. Finally, the analysis results for structural state condition 5 will be compared with the analysis results for structural state condition 6 to demonstrate the capability of the proposed technique in locating damage that only induces changes in the characteristics of the system's linear components.

It is worth noting that the applied sinusoidal input excitation with a given amplitude in each experiment as shown in Table 5 is the signal generated by a computer which was used to control the shaker's force output. However, real experimental data show that the force literally measured by the force transducer is not only different from the sinusoidal signal in amplitude due to scaling etc effects but also contains harmonics due to the inherent nonlinear nature of shaker dynamics. Therefore, in the present study, when the proposed technique was applied to analyze the experimental data, the range of frequencies of the input force excitation that was actually used in the analysis covers not only the frequency of the applied sinusoidal input but also its harmonics.

### 6.3 The results of experimental data analysis

Tables 6, 7 and 8 show the comparison of the experimental data analysis results for structural state conditions 1 and 2, 3 and 4, and 5 and 6, respectively.

Because the test rig is a 4DOF structure,  $n=4$ .  $\bar{E}_{i,i+1}$ ,  $i=1,2,3$ , was evaluated to determine the location of the system nonlinearity; and  $n-1=3$  NOFRF transmissibility results, i.e.,  $|T_{12}^{NL}(j\omega)|$ ,  $|T_{23}^{NL}(j\omega)|$ ,  $|T_{34}^{NL}(j\omega)|$  were evaluated over the frequencies of interest.

Due to the nonlinear effects of shaker dynamics as mentioned above, the range of frequencies of the excitation force literally applied to the structure covers not only the frequency of the sinusoids generated by the shaker control computer but also its

harmonics. Because of this, in the present study, index IND1 was determined from equation (30) with  $n=4$ ,  $Q=9$ ,  $\omega_1 = \Omega$  and  $\omega_2 = 10\Omega$ . Here,  $\Omega$  is the frequency of the sinusoidal signal generated by the shaker control computer. In Experiments #1 and #2, for example,  $\Omega = 2 \times \pi \times 60$  rad/s. In addition, the values of the NOFRF transmissibility over the frequencies up to the fifth harmonic were evaluated for each case.

### **Comparison of the analysis results for structural state conditions 1 and 2**

The results of IND1 in Table 6 show that the test rig under structural state condition 2 behaves considerably more nonlinearly than in structural state condition 1 and, if choosing  $\varepsilon_1 = 5 \times 10^{-4}$ , it can be concluded from Step (ii) of the proposed technique that the test rig is a linear system under structural state condition 1 but a nonlinear one under structural state condition 2. The conclusion is obviously correct as, under structural state condition 2, a nonlinear effect was introduced into the 4DOF structural system via fitting a center column and bumper on the ground floor with a 0.13mm gap between the column and bumper. This indicates that the existence of a system nonlinearity can effectively be detected by the proposed technique. In addition, if  $\varepsilon_2$  in Step (iii) of the proposed technique is chosen as  $\varepsilon_2 = 0.3$ , then from  $\bar{E}_{i,i+1}$ ,  $i = 1, 2, 3$  evaluated under structural state condition 2, it can readily be concluded that the system nonlinear component was located between masses 2 and 3, i.e., on the ground floor, which is again a correct analysis result. It is worth noting that in the experimental studies reported in this paper, this  $\varepsilon_2$  was selected by observing the obtained data analysis results. In practice a principled method based on the statistics of  $\bar{E}_{i,i+1}$ ,  $i = 1, 2, 3$  may need to be used to set this threshold.

A comparison of the NOFRF transmissibility results evaluated for state conditions 1 and 2 shows that overall the two sets of results are different. This is believed to be due to the effects of inherent, but not very significant, nonlinearity in the three-storey building structure; otherwise the  $|T_{12}^{NL}(\cdot)|$  and  $|T_{23}^{NL}(\cdot)|$  results should be very similar under the two state conditions as they are theoretically the same. Evidence of the inherent structural nonlinearity is in the value of IND1 under state condition 1 which is much smaller than the IND1 under state condition 2 but can obviously not be considered to be

zero like the IND1 in Table 1, the result obtained from a simulation study. However, it can be observed that the results of the NOFRF transmissibility at the base frequency, that is,  $|T_{12}^{NL}(j2 \times \pi \times 60)|$  and  $|T_{23}^{NL}(j2 \times \pi \times 60)|$  under the two different state conditions are basically similar. This confirms the theoretical analysis to a certain extent and implies that, in similar practical situations, the NOFRF transmissibility results evaluated at the base frequency should be used to assess any changes in system linear components to detect and locate system linear damage. Other experimental data analyses also confirm this observation.

#### **Comparison of the analysis results for structural state conditions 3 and 4**

The two values of IND1 in Table 7 are all considerably larger than  $\varepsilon_1 = 5 \times 10^{-4}$ . Therefore, based on the proposed technique, the 4DOF structural system was nonlinear under both structural state conditions 3 and 4. In addition, because  $\bar{E}_{1,2}$  is less than  $\varepsilon_2 = 0.3$ , and  $\bar{E}_{2,3}$  and  $\bar{E}_{3,4}$  are all larger than this  $\varepsilon_2$ , Step (iii) of the proposed technique indicates that the system nonlinear component was located between masses 2 and 3, i.e., on the first floor. These were, as described in Table 5, exactly the situations of the 4DOF structure under structural state conditions 3 and 4.

A comparison of the values of the NOFRF transmissibility evaluated for state condition 3 and state condition 4 as given in Table 7, shows a considerable difference between the conditions of the structural linear components. The relative difference between the NOFRF transmissibility values under the two different state conditions (averaged over the results evaluated at the five harmonic frequencies) is 52.75% for  $|T_{1,2}^{NL}(\cdot)|$ , 38.34% for  $|T_{2,3}^{NL}(\cdot)|$ , and 21.04% for  $|T_{3,4}^{NL}(\cdot)|$ , respectively. This is as expected because, compared with state condition 4, four mass blocks were added on the top of the building structure under state condition 3, which increases the value of parameter  $m_1$  in the system model. It can be analytically shown that the change of the system parameter  $m_1$  can be reflected by the values of all NOFRF transmissibilities in the system. Therefore, in addition to a nonlinear damage, a change in the linear characteristic of the system is also effectively detected.

**Comparison of the analysis results for structural state conditions 5 and 6**

From the results of IND1 and  $\bar{E}_{i,i+1}$ ,  $i = 1, 2, 3$  in Table 8, the same conclusions as those reached above about the linear/nonlinear nature of the system behaviors, and the location of the system nonlinear component can be reached for the 4DOF structural system under structural state conditions 5 and 6, which are also correct.

A comparison of the values of the NOFRF transmissibility evaluated for state condition 5 and state condition 6 as given in Table 8, however, shows a different situation. The relative difference between the NOFRF transmissibility values under the two different state conditions (again averaged over the results evaluated at the five harmonic frequencies) is 7.99% for  $|T_{1,2}^{NL}(\cdot)|$ , 7.51% for  $|T_{2,3}^{NL}(\cdot)|$ , and 20.62% for  $|T_{3,4}^{NL}(\cdot)|$ , respectively. Compared with the 52.75% difference between the two sets of  $|T_{1,2}^{NL}(\cdot)|$  results in Table 7, the 7.99% difference between the  $|T_{1,2}^{NL}(\cdot)|$  results under state conditions 5 and 6 is much less significant. In addition, apart from  $|T_{1,2}^{NL}(j2 \times \pi \times 30)|$ , the  $|T_{1,2}^{NL}(\cdot)|$  results under the two different state conditions have very little difference. Because the observed difference between the  $|T_{1,2}^{NL}(j2 \times \pi \times 30)|$  results under state conditions 5 and 6 can be explained to be due to noise and other factors, the experimental results in Table 8 basically show that compared with the data analysis results for state condition 5, the analysis result  $|T_{1,2}^{NL}(\cdot)|$  for state condition 6 almost has no change, but the analysis result  $|T_{3,4}^{NL}(\cdot)|$  for state condition 6 has a relatively significant change. These observations can be confirmed by theoretical analyses. Compared with state condition 5, three mass blocks were added on the ground floor of the structure under state condition 6, and this in fact increases the value of parameter  $m_4$  in the system model. It can be shown that the NOFRF transmissibility  $|T_{1,2}^{NL}(\cdot)|$  only depends on  $c_1, c_2, k_1, k_2$ , and  $m_1$  so that, in theory, the values of  $|T_{1,2}^{NL}(\cdot)|$  can not be affected by the increase of  $m_4$ . It can also be proved that for the 4DOF system in Fig.4, when the nonlinear component is located between masses 2 and 3,  $m_4$  will affect

the value of  $|T_{3,4}^{NL}(\cdot)|$ . Therefore, the data analysis results in Table 8 can be well-justified.

#### **Further discussions for the data analyses**

The NOFRF transmissibility analysis results in Table 7 show that compared to state condition 4, more masses are added on the top floor in state condition 3; The results in Table 8 indicate that compared to state condition 5, more masses are added on the ground floor in state condition 6. Therefore, if the mass change represents a linear damage, the proposed technique has, in these cases, not only detected the damage but also found its location.

All the results shown in Tables 6-8 and discussed above, show that the experimental data analysis conducted using the proposed technique can effectively distinguish the different state conditions of the 4DOF experimental structural system and, neglecting the effects of unavoidable noise, un-modeled dynamics, and particularly the inherent but relatively insignificant system nonlinearity, the data analysis results are also consistent with theoretical analyses. The experimental studies therefore demonstrate the effectiveness of the proposed technique in detecting and locating system nonlinearity and in evaluating changes in the characteristic parameters of the system linear components using the NOFRF transmissibility concept. Because the system nonlinearity and changes in system linear components can represent different kinds of damage in practical MDOF structural systems, the proposed technique has considerable potential to be applied in damage detection and location on real engineering structures.

## **7. Conclusions**

In the present study, the concept of the transmissibility of the NOFRFs has been proposed for a class of nonlinear MDOF structural systems. The NOFRF transmissibility is based on the recently proposed NOFRF concept, and extends the transmissibility concept for linear systems to the nonlinear case. An NOFRF transmissibility based technique is then developed for the detection and location of damage in MDOF structural systems. Both simulation and experimental studies have been conducted. The results verify the effectiveness of proposed technique and demonstrate that the technique has the potential to be applied in practice to detect and

locate damage in a wide range of MDOF engineering structural systems. Although, the MDOF system model considered in the present study is of a relatively simple form, the basic ideas can be extended to much more complicated cases including systems where there are more than one nonlinear components and/or the motion of each mass is of a multi-dimensional nature. Further research studies will focus on addressing these issues. More comprehensive experimental studies will also be conducted to investigate how to effectively apply the basic idea of the proposed technique to the health monitoring of a wide range of real engineering components and structures including beams, plates, shafts, and bridges.

## Appendix

Proof of Proposition 2:

Rewrite equation (16) as follows

$$X_i(j\omega) = \sum_{\bar{n}=1}^N G_{(i,\bar{n})}(j\omega)U_{\bar{n}}(j\omega) + T_{i,k}^{NL}(j\omega)X_k(j\omega) - T_{i,k}^{NL}(j\omega)X_k(j\omega) \quad (\text{A.1})$$

Substituting equation (17) into (A.1) for the  $X_k(j\omega)$  inside the third term on the right hand side of this equation, and taking into account equation (20) yield

$$\begin{aligned} X_i(j\omega) &= [G_{(i,1)}(j\omega) - T_{i,k}^{NL}(j\omega)G_{(k,1)}(j\omega)]U_1(j\omega) + T_{i,k}^{NL}(j\omega)X_k(j\omega) \\ &= E_{i,k}(j\omega)U_1(j\omega) + T_{i,k}^{NL}(j\omega)X_k(j\omega) \end{aligned} \quad (\text{A.2})$$

Because  $T_{i,k}^{NL}(j\omega)$ ,  $G_{(i,1)}(j\omega)$ ,  $G_{(k,1)}(j\omega)$  are all independent of the system input, equation (A.2) implies that if system (15) is excited by two different force inputs with their spectra being  $U^{(1)}(j\omega)$  and  $U^{(2)}(j\omega)$  respectively, then the corresponding spectra of the displacement responses of masses  $i$  and  $k$ , denoted by  $X_i^{(q)}(j\omega)$  and  $X_k^{(q)}(j\omega)$ ,  $q=1,2$ , can be described as

$$\begin{cases} X_i^{(1)}(j\omega) = E_{i,k}(j\omega)U^{(1)}(j\omega) + T_{i,k}^{NL}(j\omega)X_k^{(1)}(j\omega) \\ X_i^{(2)}(j\omega) = E_{i,k}(j\omega)U^{(2)}(j\omega) + T_{i,k}^{NL}(j\omega)X_k^{(2)}(j\omega) \end{cases} \quad (\text{A.3})$$

Therefore,

$$\begin{bmatrix} E_{i,k}(j\omega) \\ T_{i,k}^{NL}(j\omega) \end{bmatrix} = \begin{bmatrix} U^{(1)}(j\omega), & X_k^{(1)}(j\omega) \\ U^{(2)}(j\omega), & X_k^{(2)}(j\omega) \end{bmatrix}^{-1} \begin{bmatrix} X_i^{(1)}(j\omega) \\ X_i^{(2)}(j\omega) \end{bmatrix} \quad (\text{A.4})$$

if matrix

$$\begin{bmatrix} U^{(1)}(j\omega), & X_k^{(1)}(j\omega) \\ U^{(2)}(j\omega), & X_k^{(2)}(j\omega) \end{bmatrix}$$

is invertible. □

## References

1. S W Doebling, C R Farrar, M B Prime, D W Shevitz, Damage identification and health monitoring of structural and mechanical systems from changes in their vibration characteristics: a literature review. Los Alamos National Laboratory report LA-13070-MS, (1996).
2. T J Johnson, D E Adams, Transmissibility as a differential indicator of structural damage, *Trans. of the ASME, Journal of Vibration and Acoustics*, Vol.124 (2002), pp634-641.
3. J E Mottershead, On the zeros of structural frequency response functions and their sensitivities, *Mechanical Systems and Signal Processing*, Vol. 12 (1998), pp 591-597.
4. J M Nichols, M Seaver, S T Trickey, M D Todd, C Olson L Overbey, Detecting nonlinearity in structural systems using the transfer entropy. *Physical Review E* 72 (2005), 046217.
5. M. Paluš, Testing for nonlinearity using redundancies: quantitative and qualitative aspects. *Physica D* **80** (1995), pp 186-205.
6. M. Paluš, V. Komarek, Z. Hrnčir, and K. Sterbova, Synchronization as adjustment of information rates: Detection from bivariate time series. *Physical Review E* 63 (2001), 046211.
7. T. Schreiber, Measuring Information Transfer, *Physical Review Letter*, Vol. 85 (2000), pp461-464.
8. A. Kaiser and T. Schreiber, Information Transfer in continuous processes. *Physica D* **166** (2002), pp43-62.
9. J.M. Nichols P. Marzocca and A. Milanese, On the use of the auto-bispectral density for detecting quadratic nonlinearity in structural systems, *Journal of Sound and Vibration* Vol. 312 (2008), pp726–735.
10. A. Rivola, P.R. White, Bispectral analysis of the bilinear oscillator with application to the detection of cracks, *Journal of Sound and Vibration* Vol. 216 (1998), pp889–910.
11. C R Farrar, K Worden, M D Todd, G Park, J Nichols, D E Adams, M T Bement, K Farinholt, Nonlinear system identification for damage detection, Los Alamos National Laboratory report LA-14353, (2007).
12. D E Adams, C R Farrar, Classifying linear and nonlinear structural damage using frequency domain ARX models, *Structure Health Monitoring*, Vol. 1 (2002), pp185–201.

13. A. Neild, P.D. Mcfadden and M.S Williams, “A discrete model of vibrating beam using time-stepping approach”, *Journal of Sound and Vibration*, Vol. 239 (2001), pp99-121.
14. T G Chondros, A D Dimarogonas, J Yao, Vibration of a beam with breathing crack, *Journal of Sound and Vibration*, Vol.239 (2001), pp57-67.
15. Jan Kicinski, *Rotor dynamics*, IFFM Publishers (2005).
16. S.D. Fassois, J.S. Sakellariou, Stochastic output error vibration-based damage detection and assessment in structures under earthquake excitation, *Journal of Sound and Vibration*, Vol. 297 (2006), pp1048–1067.
17. C.R. Farrar and S.W. Doebling, Lessons Learned from Applications of Vibration Based Damage Identification Methods to Large Bridge Structures, *Proc. of the International Workshop on Structural Health Monitoring*, Stanford, CA, Sept 1997, pp. 351-370.
18. H. Zhu, M. Wu, The Characteristic receptance method for damage detection in large Mono-coupled Periodic structures, *Journal of Sound and Vibration*, Vol.251 (2002), pp241-259..
19. S. D. Fassois, J.S. Sakellariou, Time-series methods for fault detection and identification in vibrating structures, *Philosophical Transactions of the Royal Society A: Mathematical, Physical and Engineering Sciences*, **365** (2007), pp**411** –448.
20. Z.Q. Lang, S.A. Billings, Energy transfer properties of nonlinear systems in the frequency domain, *International Journal of Control*. Vol.78 (2005), pp354–362.
21. Z Q Lang, Z K Peng, A novel approach for nonlinearity detection in vibrating systems, *Journal of Sound and Vibration*, Vol. 314 (2008), pp603-615.
- 22 Z K Peng, Z Q Lang, S A Billings, Novel method for detecting the non-linear components in periodic structures, *Proc. IMechE Vol. 222* (2008), Part C: J. Mechanical Engineering Science, pp903-019.
23. Z K Peng, Z Q Lang, Detecting the position of non-linear component in periodic structures from the system responses to dual sinusoidal excitations. *International Journal of Non-Linear Mechanics*, Vol. 42 (2007), pp1074 – 1083.
24. Z. Q. Lang, S. A. Billings, Output frequency characteristics of nonlinear systems, *International Journal of Control*, Vol. **64** (1996), pp1049-1067.
25. I W Sandberg, A perspective on System Theory, *IEEE Transactions on Circuits and Systems*, Vol. CAS-31 (1984), pp88-103.
26. Z.K Peng, Z.Q Lang, S.A Billings, Nonlinear Output Frequency Response Functions of MDOF Systems with Multiple Nonlinear Components, *International Journal of Non-linear Mechanics*, Vol. 42 (2007), 941-958.

27. Z.K Peng, Z.Q Lang, F L Chu, G Meng, Locating Nonlinear Components in Periodic Structures Using the Nonlinear Effects, *Structure Health Monitoring*, in Press (2010).
28. Peng, Z K, **Lang, Z Q**, Billings, S A, Nonlinear output frequency response functions for multi-input nonlinear Volterra systems. *International Journal of Control*, Vol.80 (2007), pp843-855.
- 29 Peng, Z K, **Lang, Z Q**, Billings, S A, Analysis of Locally Nonlinear MDOF Systems Using Nonlinear Output Frequency Response Functions. *Journal of Vibration and Acoustics*, In press (2010).
30. Peng Z K, **Lang Z Q**, Chu F L, Numerical analysis of cracked beams using nonlinear output frequency response functions , *Computers & Structure*, Vol.86 (2008), pp1809-1818.
31. <http://institute.lanl.gov/ei/structural-health-monitoring/test-structures-applications/>

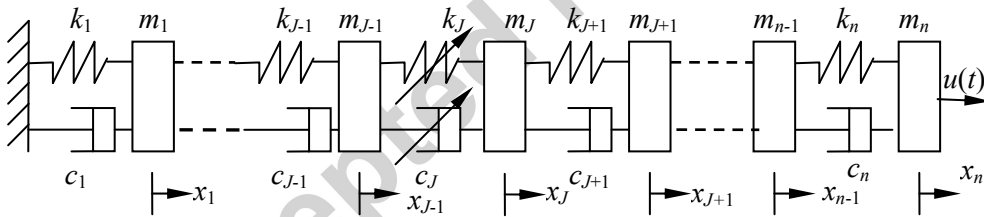


Figure 1 The MDOF structural system considered in the present study

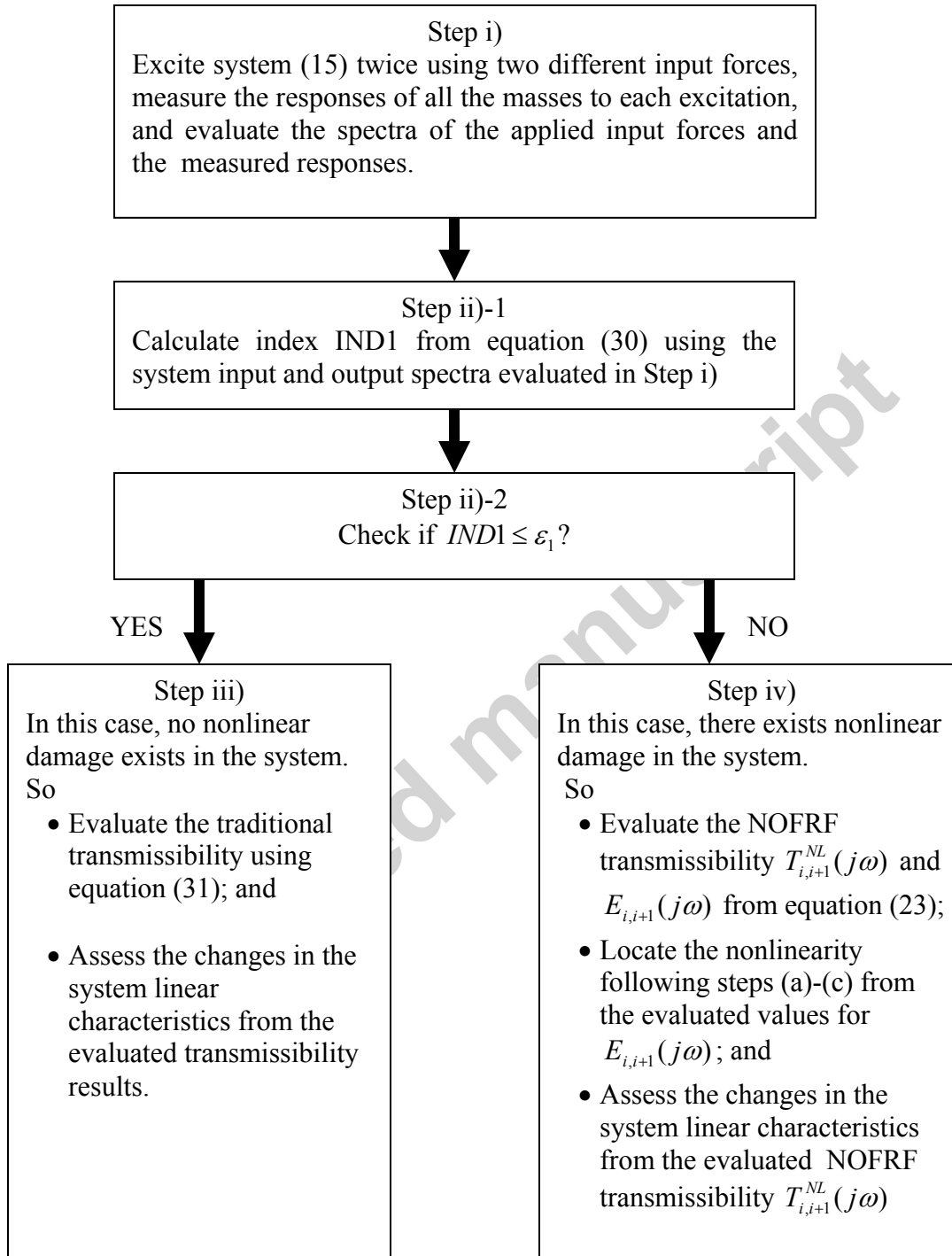


Figure 2 A flow chart of the NOFRF transmissibility-based MDOF system damage detection and location technique

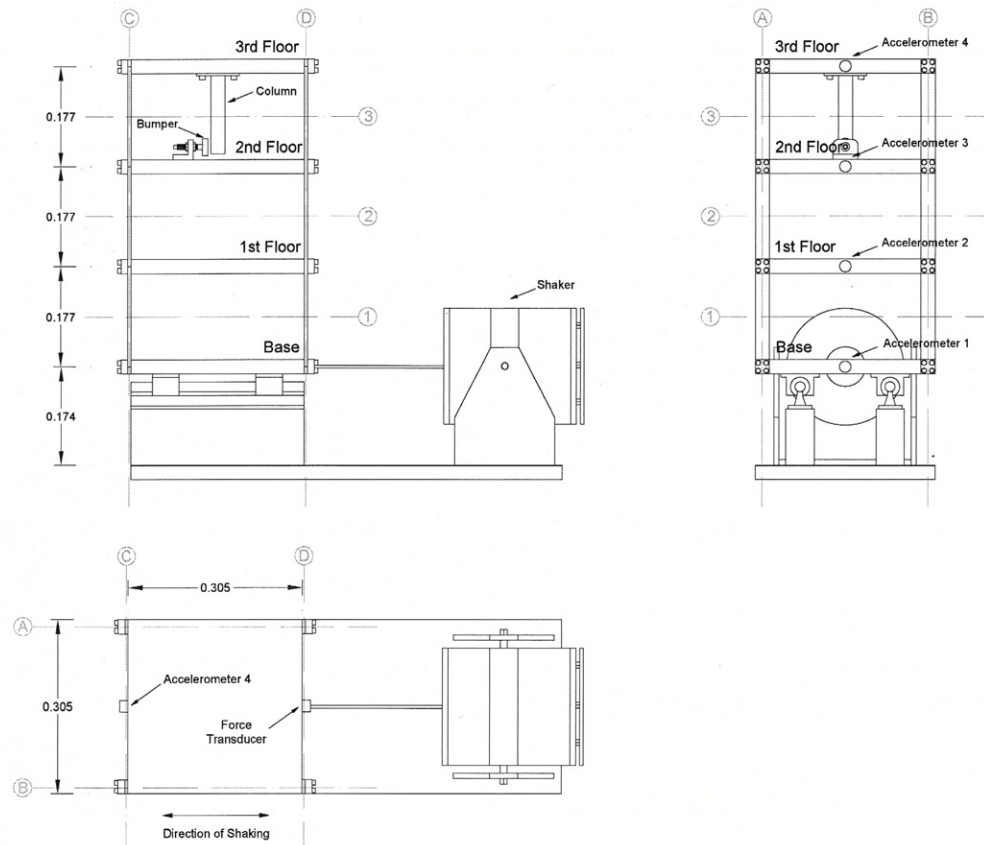


Figure 3 Schematic representation of a three-storey building structure used for the experimental studies

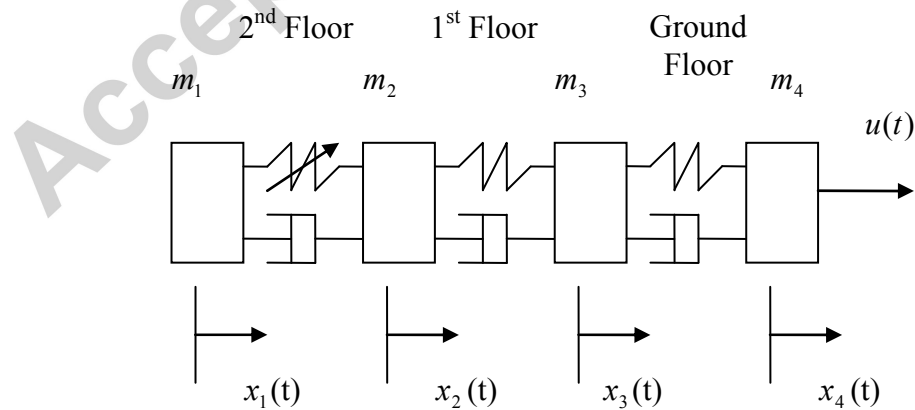


Figure 4 The 4DOF system model of the three storey building structure

**Table 1 Analysis Results for Case I of Simulation Studies**

System Characteristics	Analysis Results	Theoretical Values
IND1	1.21e-010	0
$E_{1,2} =  E_{1,2}(j2 \times \pi \times 20) $	NA	NA
$E_{2,3} =  E_{2,3}(j2 \times \pi \times 20) $		
$\bar{E}_{1,2} = E_{1,2} / \max(E_{1,2}, E_{2,3})$		
$\bar{E}_{2,3} = E_{2,3} / \max(E_{1,2}, E_{2,3})$		
$ T_{1,2}^{NL}(j\omega)  =  T_{1,2}^{NL}(j2 \times \pi \times 20) $	0.543	0.543
$ T_{2,3}^{NL}(j\omega)  =  T_{2,3}^{NL}(j2 \times \pi \times 20) $	0.758	0.758

**Table 2 Analysis Results for Case II of Simulation Studies**

System Characteristics	Analysis Results	Theoretical Values
IND1	2.02e-004	>0
$E_{1,2} =  E_{1,2}(j2 \times \pi \times 20) $	0.00000000192	0
$E_{2,3} =  E_{2,3}(j2 \times \pi \times 20) $	0.0000431	4.31e-005
$\bar{E}_{1,2} = E_{1,2} / \max(E_{1,2}, E_{2,3})$	0.0000445	0
$\bar{E}_{2,3} = E_{2,3} / \max(E_{1,2}, E_{2,3})$	1.000	1
$ T_{1,2}^{NL}(j\omega)  =  T_{1,2}^{NL}(j2 \times \pi \times 20) $	0.543	0.543
$ T_{2,3}^{NL}(j\omega)  =  T_{2,3}^{NL}(j2 \times \pi \times 20) $	0.681	0.681

**Table 3 Analysis Results for Case III of Simulation Studies**

System Characteristics	Analysis Results	Theoretical Values
IND1	1.93e-004	>0
$E_{1,2} =  E_{1,2}(j2 \times \pi \times 20) $	0.00000000224	0
$E_{2,3} =  E_{2,3}(j2 \times \pi \times 20) $	0.0000387	3.87 e-005
$\bar{E}_{1,2} = E_{1,2}/\max(E_{1,2}, E_{2,3})$	0.0000578	0
$\bar{E}_{2,3} = E_{2,3}/\max(E_{1,2}, E_{2,3})$	1.000	1
$ T_{1,2}^{NL}(j\omega)  =  T_{1,2}^{NL}(j2 \times \pi \times 20) $	0.584	0.584
$ T_{2,3}^{NL}(j\omega)  =  T_{2,3}^{NL}(j2 \times \pi \times 20) $	0.611	0.611

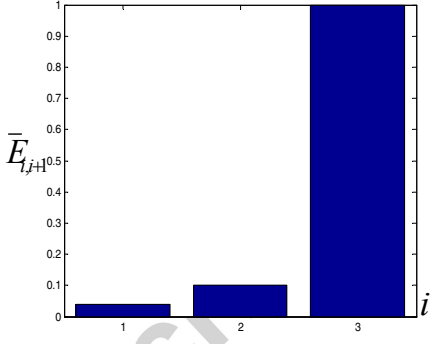
**Table 4 Analysis Results for Case IV of Simulation Studies**

System Characteristics	Analysis Results	Theoretical Values
IND1	6.49e-004	>0
$E_{1,2} =  E_{1,2}(j2 \times \pi \times 20) $	0.00000000156	0
$E_{2,3} =  E_{2,3}(j2 \times \pi \times 20) $	0.0000431	4.31e-005
$\bar{E}_{1,2} = E_{1,2}/\max(E_{1,2}, E_{2,3})$	0.0000361	0
$\bar{E}_{2,3} = E_{2,3}/\max(E_{1,2}, E_{2,3})$	1.000	1
$ T_{1,2}^{NL}(j\omega)  =  T_{1,2}^{NL}(j2 \times \pi \times 20) $	0.543	0.543
$ T_{2,3}^{NL}(j\omega)  =  T_{2,3}^{NL}(j2 \times \pi \times 20) $	0.680	0.681

**Table 5 Details of the Experiments**

Experiment	Input excitation applied by shaker control computer	Structural state condition under which experiment was conducted
Experiment #1	60Hz sinusoidal with amplitude 3	<b>State Condition 1</b> The center column and bumper were fitted on the ground floor but Gap was so large that no nonlinearity was introduced to the structure.
Experiment #2	60Hz sinusoidal with amplitude 6	
Experiment #3	60Hz sinusoidal with amplitude 4	<b>State Condition 2</b> The center column and bumper were fitted on the ground floor and Gap=0.13mm.
Experiment #4	60Hz sinusoidal with amplitude 6	
Experiment #5	40Hz sinusoidal with amplitude 2	<b>State Condition 3</b> * The center column and bumper were fitted on the 1 <sup>st</sup> floor and Gap=0.13mm; * 50% stiffness reduction in the two columns located between the ground and first floors, and in the intersections of plane B with planes C and D; * 4 mass blocks were added to the top floor.
Experiment #6	40Hz sinusoidal with amplitude 3.5	
Experiment #7	40Hz sinusoidal with amplitude 2	<b>State Condition 4</b> * The center column and bumper were fitted on the 1 <sup>st</sup> floor and Gap =0.13mm; * 50% stiffness reduction in the two columns located between the base and first floor, and in the intersections of plane B with planes C and D;
Experiment #8	40Hz sinusoidal with amplitude 3.5	
Experiment #9	30Hz sinusoidal with amplitude 2	<b>State Condition 5</b> The center column and bumper were fitted on the 1 <sup>st</sup> floor and Gap =0.13mm;
Experiment #10	30Hz sinusoidal with amplitude 4	
Experiment #11	30Hz sinusoidal with amplitude 2	<b>State Condition 6</b> * The center column and bumper were fitted on the 1 <sup>st</sup> floor and Gap =0.13mm; * 3 mass blocks were added to the ground floor.
Experiment #12	30Hz sinusoidal with amplitude 4	

**Table 6 Comparison of the Real Data Analysis Results  
for Structural State Conditions 1 and 2**

	The experimental data analysis results for the test rig under <b>State Condition 1</b>	The experimental data analysis results for the test rig under <b>State Condition 2</b>
IND1	<u><b>9.21e-005</b></u>	<u><b>5.80e-003</b></u>
$\bar{E}_{i,i+1}, i = 1, 2, 3$	N/A	
$ T_{12}^{NL}(j2 \times \pi \times 60) $	<u><b>0.7450</b></u>	<u><b>0.7667</b></u>
$ T_{12}^{NL}(j2 \times \pi \times 120) $	0.1917	0.3068
$ T_{12}^{NL}(j2 \times \pi \times 180) $	2.4399	0.8164
$ T_{12}^{NL}(j2 \times \pi \times 240) $	0.9012	0.4619
$ T_{12}^{NL}(j2 \times \pi \times 300) $	0.3355	0.1771
$ T_{23}^{NL}(j2 \times \pi \times 60) $	<u><b>3.6518</b></u>	<u><b>4.2531</b></u>
$ T_{23}^{NL}(j2 \times \pi \times 120) $	2.0257	0.3682
$ T_{23}^{NL}(j2 \times \pi \times 180) $	0.3341	0.1391
$ T_{23}^{NL}(j2 \times \pi \times 240) $	0.7128	0.1850
$ T_{23}^{NL}(j2 \times \pi \times 300) $	0.6353	0.1909
$ T_{34}^{NL}(j2 \times \pi \times 60) $	0.2199	0.4250
$ T_{34}^{NL}(j2 \times \pi \times 120) $	0.1704	0.7321
$ T_{34}^{NL}(j2 \times \pi \times 180) $	0.0757	1.4025
$ T_{34}^{NL}(j2 \times \pi \times 240) $	0.0615	2.1753
$ T_{34}^{NL}(j2 \times \pi \times 300) $	0.0523	0.9910

**Table 7 Comparison of the Real Data Analysis Results  
for Structural State Conditions 3 and 4**

	The experimental data analysis results for the test rig under Status <b>State condition 3</b>	The experimental data analysis results for the test rig under Status <b>State condition 4</b>
IND1	<u><b><math>5.6000e-3</math></b></u>	<u><b><math>9.9000e-3</math></b></u>
$\bar{E}_{i,i+1}, i = 1, 2, 3$		
$ T_{12}^{NL}(j2 \times \pi \times 40) $	<u><b>0.5828</b></u>	<u><b>0.2410</b></u>
$ T_{12}^{NL}(j2 \times \pi \times 80) $	<u><b>0.3937</b></u>	<u><b>0.6468</b></u>
$ T_{12}^{NL}(j2 \times \pi \times 120) $	<u><b>0.1896</b></u>	<u><b>0.1756</b></u>
$ T_{12}^{NL}(j2 \times \pi \times 160) $	<u><b>0.0687</b></u>	<u><b>0.0275</b></u>
$ T_{12}^{NL}(j2 \times \pi \times 200) $	<u><b>0.0750</b></u>	<u><b>0.0199</b></u>
$ T_{23}^{NL}(j2 \times \pi \times 40) $	1.1071	2.0952
$ T_{23}^{NL}(j2 \times \pi \times 80) $	0.7193	0.5273
$ T_{23}^{NL}(j2 \times \pi \times 120) $	0.7778	0.8723
$ T_{23}^{NL}(j2 \times \pi \times 160) $	2.8102	3.3609
$ T_{23}^{NL}(j2 \times \pi \times 200) $	0.6612	0.9521
$ T_{34}^{NL}(j2 \times \pi \times 40) $	0.5177	0.5398
$ T_{34}^{NL}(j2 \times \pi \times 80) $	9.3953	8.0210
$ T_{34}^{NL}(j2 \times \pi \times 120) $	4.3623	4.5555
$ T_{34}^{NL}(j2 \times \pi \times 160) $	5.4426	9.8445
$ T_{34}^{NL}(j2 \times \pi \times 200) $	16.5217	16.6871

**Table 8 Comparison of the Real Data Analysis Results  
for Structural State Conditions 5 and 6**

	The experimental data analysis results for the test rig under Status <b>State Condition 5</b>	The experimental data analysis results for the test rig under Status <b>State Condition 6</b>
IND1	<u><b>0.0600</b></u>	<u><b>0.0480</b></u>
$\bar{E}_{i,i+1}, i = 1, 2, 3$		
$ T_{12}^{NL}(j2 \times \pi \times 30) $	<u><b>1.5419</b></u>	<u><b>1.0999</b></u>
$ T_{12}^{NL}(j2 \times \pi \times 60) $	<u><b>0.4820</b></u>	<u><b>0.4577</b></u>
$ T_{12}^{NL}(j2 \times \pi \times 90) $	<u><b>0.2338</b></u>	<u><b>0.2264</b></u>
$ T_{12}^{NL}(j2 \times \pi \times 120) $	<u><b>0.1314</b></u>	<u><b>0.1349</b></u>
$ T_{12}^{NL}(j2 \times \pi \times 150) $	<u><b>0.1427</b></u>	<u><b>0.1433</b></u>
$ T_{23}^{NL}(j2 \times \pi \times 30) $	2.5731	2.2744
$ T_{23}^{NL}(j2 \times \pi \times 60) $	1.5412	1.8118
$ T_{23}^{NL}(j2 \times \pi \times 90) $	1.0208	1.0460
$ T_{23}^{NL}(j2 \times \pi \times 120) $	1.1157	1.1059
$ T_{23}^{NL}(j2 \times \pi \times 150) $	1.1947	1.1344
$ T_{34}^{NL}(j2 \times \pi \times 30) $	0.2490	0.3771
$ T_{34}^{NL}(j2 \times \pi \times 60) $	2.3993	2.3324
$ T_{34}^{NL}(j2 \times \pi \times 90) $	11.2686	8.6609
$ T_{34}^{NL}(j2 \times \pi \times 120) $	6.5080	8.1805
$ T_{34}^{NL}(j2 \times \pi \times 150) $	2.8338	2.8334